# Simulating three-dimensional turbulence with SPH

**By S. Adami†, X.Y. Hu† AND N.A. Adams†**

In this paper, we have investigated the ability of smoothed particle hydrodynamics (SPH) to simulate turbulent flows. It is well known that the standard method without corrections cannot predict the energy cascade of a turbulent flow. In the absence of viscosity, standard SPH simulations produce purely noisy particle motion and at finite viscosities the method overpredicts dissipation. As a remedy, we have introduced a modified transport velocity to advect particles that homogenizes the particle distribution, thus stabilizing the numerical scheme. In addition, artificial dissipation is strongly reduced, and we successfully applied the new method to transitional flows. Here, we present two- and three-dimensional simulation results of the Taylor-Green vortex flow. We analyzed the energy spectra and dissipation rates and found good agreement with DNS data from the literature.

## 1. Introduction

Presented independently by Lucy (1977) and Gingold & Monaghan (1977), smoothed particle hydrodynamics (SPH) was first introduced with the aim of simulating astrophysical problems where its grid-less nature is obviously advantageous. But over the years, SPH was successfully applied to many other fields ranging from structural mechanics to complex multi-phase flows with transport models of surface active agents (Monaghan 2005; Adami *et al.* 2010).

Turbulence modeling with SPH is still a rather new area of research. The difficulty of the standard method for this application is two-fold. On one hand, in the absence of physical viscosity, i.e., when solving the Euler equations with SPH, by the nature of the method conservation of energy implies negligible numerical dissipation that finally drives the flow to a randomly fluctuating system. On the other hand, when solving the Navier-Stokes equation at finite Reynolds number, the violation of gauge invariance by the pressure-term discretization in the conservative form introduces additional numerical dissipation that can be comparable to the physical viscous dissipation and damp the flow excessively.

In 2002 Monaghan showed a Lagrangian-averaged Navier-Stokes turbulence model-type modification of the original SPH method and simulated two-dimensional turbulence. Although achieving good results, this method was shown to be computationally very inefficient (Mansour 2007). Violeau & Issa (2007) presented three different turbulence models for SPH, two algebraic models and one based on the Reynolds stress model. They applied their method to two-dimensional open channel turbulent flows and two-dimensional collapsing water column and could improve the quality of the benchmark results compared with those of the original SPH. But compared to state-of-the-art results with a grid-based method the comparison was still poor. Dalrymple & Rogers (2006)

† Institute of Aerodynamics and Fluid Mechanics, Technische Universität München

simulated two-dimensional breaking waves with SPH using a LES-type turbulence model. Robinson & Monaghan (2012) and Mansour (2007) studied how well SPH performs in a direct numerical simulation (DNS). They show that the original SPH method can reproduce the (inverse) energy cascade but their work is still limited to two-dimensional problems. Ellero *et al.* (2010) and Shi *et al.* (2012) showed that SPH in its original form has an effective implicit viscosity and some characteristics of turbulent flows when applied to high Mach number, isentropic homogeneous flows.

In this work we present a novel SPH method to simulate turbulent flows. Based on the standard SPH formulation (Monaghan 2005; Hu & Adams 2006) we introduce a transport velocity different from the momentum velocity to advect particles. Such a modification was first proposed by Monaghan (1989), who used a kernel-based smoothing of the flow field to advect particles and showed that his *XSPH* method is very similar to a Lagrangian-averaged Navier-Stokes turbulence model (Chen *et al.* 1998; Holm 1999). Different from XSPH and similar methods, we solve a modified momentum equation including a constant background pressure field that regularizes particle motion in a physically consistent way while strongly reducing artificial numerical dissipation. Details of this method are given in the next section and our two- and three-dimensional results show that SPH is capable of simulating turbulent flows.

## 2. Numerical method

In this section we briefly introduce the governing equations for a Newtonian fluid and introduce briefly the SPH framework.

### 2.1. *Governing equations*

The isothermal Navier-Stokes equations are solved in a Lagrangian frame of reference. Thus, mass conservation gives

$$\frac{d\rho}{dt} = -\rho \nabla \cdot \mathbf{v} \ , \tag{2.1}$$

where $\rho$ is the density of the fluid and $\mathbf{v}$ is the velocity vector. In the absence of body forces, the momentum equation reads

$$\frac{d\mathbf{v}}{dt} = -\frac{1}{\rho}\nabla p + \nu \nabla^2 \mathbf{v} \ . \tag{2.2}$$

Here, $p$ denotes the pressure and $\nu$ is the kinematic viscosity ($\nu = \eta/\rho$ with the dynamic viscosity $\eta$).

### 2.2. *SPH Discretization*

In SPH, Lagrangian particles are used to discretize the computational domain and each of these particles carries a portion of the total mass and momentum. The field variables at the particle positions are smoothed with a kernel, $W$, and the acceleration of each point results from particle-particle interactions. Following Hu & Adams (2006), the density of each particle, $i$, is calculated with a summation over all neighboring particles, $j$,

$$\rho_i = m_i \sum_j W_{ij} \tag{2.3}$$

with the local kernel estimate $W_{ij} = W\left(|\mathbf{r_i} - \mathbf{r_j}|, h\right)$. This form conserves the mass of each particle exactly and $\sum_j W_{ij}$ is the inverse of the particle volume. Although not

considered in this work, this summation allows for density discontinuities in multi-phase flows. To avoid a computationally expensive pressure-poisson solver, we treat the fluid weakly compressible with an equation-of-state that relates the density to a pressure, $p$,

$$p(\rho) = c_s^2(\rho - \rho_0) \ . \tag{2.4}$$

The sound speed, $c_s$, is chosen based on a scale-analysis (Morris *et al.* 1997) to ensure a maximum admissible density variation. Usually this threshold is 1% and $c_s$ is ten times the reference velocity. This form is equivalent to the classical SPH equation-of-state with $\gamma = 1$ and no background pressure. The acceleration of a particle due to a pressure gradient and viscous shear forces is

$$\frac{d\mathbf{v_i}}{dt}^{(p)} = -\frac{1}{m_i}\sum_j \left(V_i^2 + V_j^2\right)\frac{p_i\rho_j + p_j\rho_i}{\rho_i + \rho_j}\nabla W_{ij} \ , \tag{2.5}$$

and

$$\frac{d\mathbf{v_i}}{dt}^{(\nu)} = -\frac{\eta}{m_i}\sum_j \left(V_i^2 + V_j^2\right)\frac{\mathbf{v_i} - \mathbf{v_j}}{r_{ij}}\frac{\partial W_{ij}}{\partial r} \ , \tag{2.6}$$

where $V$ is the volume of a particle, $\nabla W_{ij} = \frac{\partial W_{ij}}{\partial r}\mathbf{e}_{ij}$ is the kernel gradient in inter-particle normal direction, $\mathbf{e}_{ij}$, and $\eta$ is the dynamic viscosity. For the details of the derivation we refer to the literature (e.g., Hu & Adams 2007).

The interpolation kernel function can be any function that approximates the Dirac delta distribution as the smoothing length, $h$, of the kernel vanishes. To limit the number of particle-particle interactions it is common practice to use a kernel with compact support. Here, we use the quintic spline kernel (Morris *et al.* 1997)

$$W(|\mathbf{r}|, h) = f_{dim}\begin{cases}(3-s)^5 - 6(2-s)^5 + 15(1-s)^5, & 0 \le s < 1;\\ (3-s)^5 - 6(2-s)^5, & 1 \le s < 2;\\ (3-s)^5, & 2 \le s < 3;\\ 0, & s \ge 3,\end{cases} \tag{2.7}$$

with the non-dimensional distance $s = |\mathbf{r}|/h$ and the normalization factor $f_{dim}$ to satisfy the identity property ($f_2 = 63/\left(478\pi r_c^2\right)$ and $f_3 = 27/\left(120\pi r_c^3\right)$). This kernel has a cutoff distance of $r_c = 3h$ and we use $\Delta x = h$ as initial particle distance.

The new modified SPH method (mSPH) takes advantage of the regularization of the particle motion owing to an additional background pressure. Typically, we use the reference pressure $p_0 = c_s^2\rho_0$ as a constant background field and compute its gradient at the particle positions. As SPH is not reproducing a constant field exactly, i.e. SPH is not gauge invariant, an additional force is exerted by this background pressure that counteracts non-homogeneous particle distributions. This correction is applied only to the acceleration of the particles but is not considered in the momentum term. Consequently, the conservation property is maintained while strongly reducing numerical dissipation. The discretized conservation equations are evolved in time using a velocity-verlet time-stepping scheme where the step size is limited by the classical CFL condition.

### 2.3. *Post-processing*

To analyze the method and compare our results against literature data, post-processing of the simulation results is necessary. Particle simulations produce scattered data and

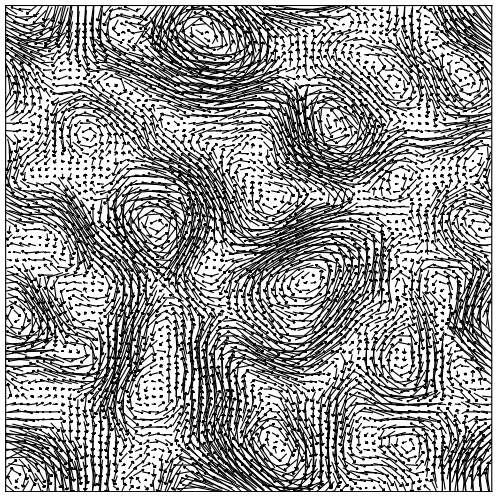

FIGURE 1. Velocity vector plot at T=2 for 8x8 TGV at $Re = \infty$.

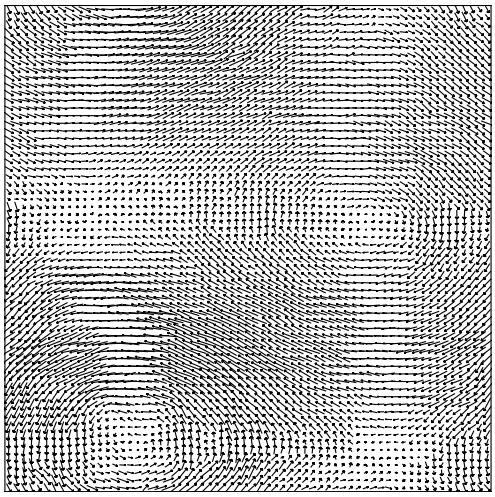

FIGURE 2. Velocity vector plot at T=30 for 8x8 TGV at $Re = \infty$.

therefore we first interpolate the data on a Cartesian grid. We have implemented and compared different interpolation schemes to eliminate interpolation artifacts. In section 3.1 we compare the results using a normalized smoothing, with the kernel function as used in the simulation and the interpolation with first and second-order moving-least-squares (Gossler 2001). Energy spectra are extracted from the interpolated grid results using the FFTW package (Frigo & Johnson 2005). Probability density functions (pdf) of the particle accelerations are obtained directly from the scattered data.

## 3. Results

The main results of our SPH simulations are presented in this section. Starting with a two-dimensional Taylor-Green vortex flow we test our developed post-processing tool and found good agreement with literature results. Also, we present the results for the break-down of a three-dimensiona Taylor-Green vortex (TGV) for different Reynolds numbers in the range of $Re = 100 - 3000$.

### 3.1. *Two-dimensional Taylor-Green vortex*

A periodic array of Cartesian particles is initialized in a rectangular box of size $L = 1$. The velocity is initialized with an exact solution of the incompressible Navier-Stokes equation given by

$$u(x, y) = -V_0 \cos(2\pi x/l_{ref}) \sin(2\pi y/l_{ref}) \tag{3.1}$$

$$v(x, y) = \quad V_0 \sin(2\pi x/l_{ref}) \cos(2\pi y/l_{ref}) \ , \tag{3.2}$$

with $l_{ref} = 0.25$. Thus, an array of 8x8 counter rotating Taylor-Green vortices is used. The density of the fluid is $\rho = 1$ and the physical viscosity is zero. Figures 1 and 2 show the velocity field of the flow at $T = 2$ and $T = 30$ from a simulation using $64^2$ particles. Note, the size of the velocity vectors was adjusted in each figure to improve the visibility.

Initially, the 8x8 array of vortices causes a strong disturbance of the flow, and at $T = 2$ the flow field is already turbulent. Similar to findings by Hu & Adams (2012)

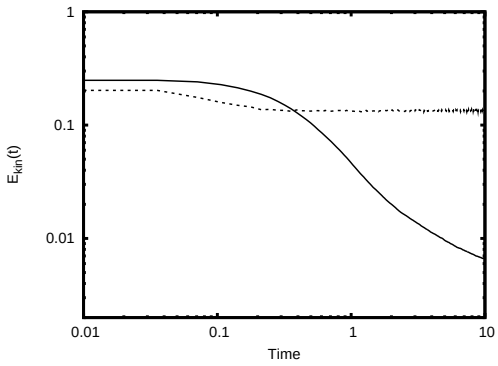


FIGURE 3. Comparison of the temporal evolution of the total kinetic energy of the 8x8 TGV between SPH (*dashed line*) and mSPH (*solid line*).

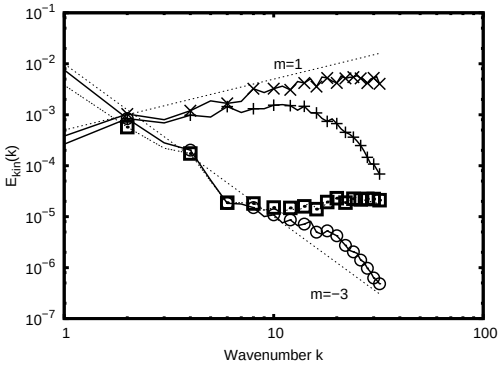


FIGURE 4. Comparison of energy spectra for the 8x8 TGV at T=10; + and x denote the standard SPH results with quintic spline and MLS interpolation; ∘ and □ denote mSPH results with quintic-spline and MLS interpolation.

we also find that two-dimensional turbulence is characterized by merging and pairing of small vortices, and at late times we observe only a single remaining pair of counter-rotating vortices, see $T = 30$. Not shown here, the standard SPH method produces a purely random flow with a noisy velocity field and does not reproduce any turbulent characteristics. A comparison of the total kinetic energy of this example using both the standard method and our approach is shown in Figure 3.

As expected, the standard SPH method conserves the kinetic energy in the absence of physical viscosity. The small decrease in the total kinetic energy is transferred to potential energy as the particles rearrange from the initial Cartesian setup, but at later times the energy is constant. The particle velocity field is very noisy and the motion is purely random. Contrarily, as shown in the velocity vector plots, mSPH dissipates energy at small scales and the total kinetic energy decays in time. Energy spectra for this example are shown in Figure 4. Here, both the standard SPH results and our new results are post-processed using the quintic-spline kernel and a second-order moving-least-squares (MLS) interpolation. At low wavenumbers both interpolation schemes give the same results, but at high wavenumbers the results differ. As expected, the spline interpolation smoothes the flow field and the resolvable energy modes at high wavenumbers are reduced. The energy spectrum of the standard SPH has a linear slope of magnitude $m = 1$ in a log-log scale that is equivalent to a purely noisy velocity field. Theoretically, two-dimensional turbulence has an energy cascade with a slope of $m = -3$ in the inertial range. Using mSPH we find a very similar cascade in the well-resolved wave number range.

### 3.2. *Three-dimensional Taylor-Green vortex*

The three-dimensional Taylor-Green vortex flow is a complex transitional flow that is laminar at early times and becomes fully turbulent with nearly isotropic small scales exhibiting a $k^{-5/3}$ inertial range in the kinetic energy spectrum. The initial velocity field is given by

$$u(x,y,z) = \quad V_0 \cos(2\pi x/L) \sin(2\pi y/L) \cos(2\pi z/L) \tag{3.3}$$

$$v(x,y,z) = -V_0 \sin(2\pi x/L) \cos(2\pi y/L) \cos(2\pi z/L) \tag{3.4}$$

$$w(x,y,z) = \quad 0\ . \tag{3.5}$$

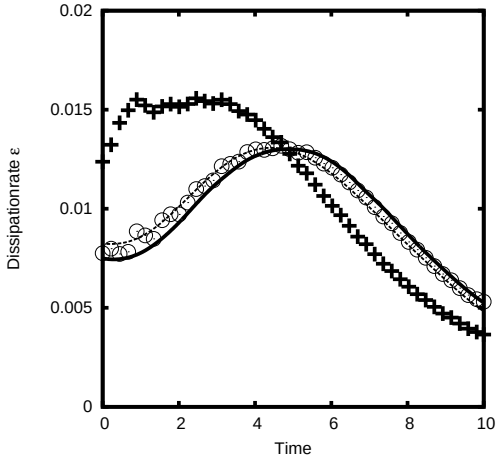


FIGURE 5. Dissipation rate at $Re = 100$ using DNS (*solid line*), Smagorinsky model (*dashed line*), standard SPH (+) and mSPH (∘).

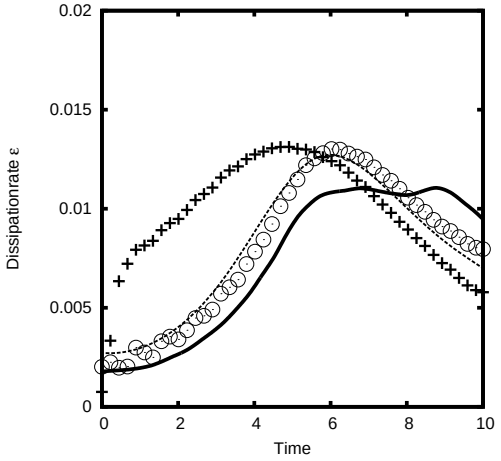


FIGURE 6. Dissipation rate at $Re = 400$ using DNS (*solid line*), Smagorinsky model (*dashed line*), standard SPH (+) and mSPH (∘).

Here, the box size $L$ is $L = 2\pi$. As in two dimensions, this flow has eight counter-rotating vortices and we simulate it for different Reynolds numbers in the range of $Re = 100 - 3000$. The Reynolds number ($Re = v_{ref}\ l_{ref}/\nu$) is calculated with the reference velocity, $v_{ref} = V_0$, the length scale, $l_{ref} = 1$, and the kinematic viscosity, $\nu = \eta/\rho$. The box is discretized with $64^3$ particles and we compare our results with DNS data of Brachet *et al.* (1983) and the conventional ($C_S = 0.18$) Smagorinsky model (Hickel *et al.* 2006). Note, the resolution of the DNS was $256^3$, and the Smagorinsky results were obtained with the same resolution as used in this work.

Looking at the dissipation rate $\varepsilon = -dE_{kin}/dt$, in Figures 5-7 we compare the results of the DNS (bold line), the standard Smagorinsky model (dashed line), the standard SPH model (+) and mSPH (∘) at different Reynolds numbers. At $Re = 100$, the flow is fully resolved at the given resolution and the Smagorinsky model gives a similar dissipation rate compared to that of the DNS but overpredicts the rate at early times. Using the standard SPH shows clearly the inability of the classical method to simulate transitional flows. Starting at $T = 0$, excessive dissipation is found and the flow is almost eliminated. In contrast, mSPH is able to reproduce the dissipation rate reasonably well. Surprisingly, the result is very close to the standard Smagorinsky model with even better agreement at early times as compared with that of the DNS. That means the corrected particle transport velocity implicitly takes effect as an eddy-viscosity model on scales below the numerical resolution.

Almost identical characteristics are found for $Re = 400$, see Figure 6. The standard SPH method completely fails in predicting this flow, mSPH recovers the transition to turbulence and the dissipation rate is slightly more accurate compared to that of the Smagorinsky model. At higher Reynolds numbers the difference between mSPH and the Smagorinsky model is even more pronounced. Figure 7 shows the dissipation rate for the same problem at $Re = 3000$. Using the Smagorinsky model, the kinetic energy decreases rapidly at excessive rates. Still different from the DNS but showing a clear tendency toward the correct result, the dissipation rate is much better predicted with the mSPH.

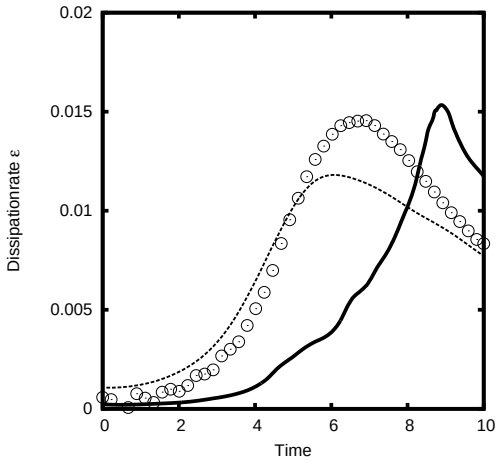


FIGURE 7. Dissipation rate at $Re = 3000$ using DNS (*solid line*), Smagorinsky model (*dashed line*) and the proposed method (○).

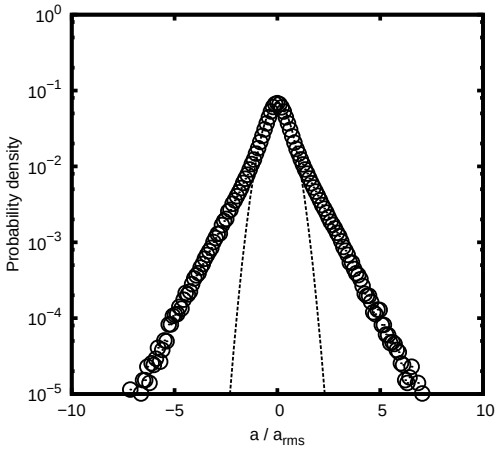


FIGURE 8. Lagrangian PDF of particle accelerations at $Re = 3000$; ○ denote simulation results and dashed line shows a Gaussian distribution.

In the initial phase the overdissipation is smaller and the peak of the maximum rate occurs closer to the expected peak with comparable magnitude.

In Fig. 8 we show the Lagrangian PDF of the particle accelerations at $Re = 3000$ of a simulation using the modified SPH method. As expected, the mean and most probable acceleration is zero and the PDF is symmetric. Comparing the PDF against a Gaussian distribution the simulated flow clearly shows intermittent behavior. This result shows the improvement of mSPH since standard SPH does not predict intermittency at low Mach numbers, see Shi *et al.* (2012).

## 4. Conclusions

We have developed a modified SPH method with a physically consistent modified transport velocity to advect the Lagrangian particles and studied the ability to predict turbulent flows. Based on promising two-dimensional results we have extended our method for three-dimensional problems and tested the method with the transitional Taylor-Green vortex flow. In two dimensions, the classical $k^{-3}$ decay in the energy spectrum is recovered and the scheme is stable even for vanishing physical viscosity. The dissipation rate of the three-dimensional TGV agrees well with low Reynolds number DNS results and compared to the standard Smagorinsky model the accuracy is improved. Also, we found intermittency in the particle accelerations at $Re = 3000$. To the best knowledge of the authors, this is the first time that a weakly compressible SPH method without complex and mostly ad hoc modifications is capable of predicting two- and three-dimensional turbulence.

## Acknowledgements

We kindly thank Dr. Christian Stemmer for providing computing resources and support with the simulations on the cluster of the Institute of Aerodynamics and Fluid Mechanics,

TU München. We also gratefully thank Daniel Price for his visualization tool *splash* that was used to generate some figures for this report (Price 2007). Also, we thank Dr. Stefan Hickel for providing reference data of the 3D TGV DNS and Smagorinsky results and Prof. J. Andrzej Domaradzki for many inspiring discussions.

## REFERENCES

Adami, S., Hu, X. & Adams, N. 2010 A conservative SPH method for surfactant dynamics. *J Comput Phys* **229** (5), 1909–1926.

Brachet, M. E., Meiron, D. I., Orszag, S. A., Nickel, B. G., Morf, R. H. & Frisch, U. 1983 Small-scale structure of the TaylorGreen vortex. *J Fluid Mech* **130**, 411–452.

Chen, S., Foias, C., Holm, D., Olson, E., Titi, E. & Wynne, S. 1998 Camassa-Holm equations as a closure model for turbulent channel and pipe flow. *Phys Rev L* **81** (24), 5338–5341.

Dalrymple, R. & Rogers, B. 2006 Numerical modeling of water waves with the SPH method. *Coastal Engin* **53** (2-3), 141–147.

Ellero, M., Español, P. & Adams, N. 2010 Implicit atomistic viscosities in smoothed particle hydrodynamics. *Phys Rev E* **82** (4).

Frigo, M. & Johnson, S. G. 2005 The Design and Implementation of FFTW3. *Proceedings of the IEEE* **93** (2), 216–231.

Gingold, R. & Monaghan, J. 1977 Smoothed particle hydrodynamics -Theory and application to non-spherical stars. *Mon. Not. R. Astron. Soc.* **181**, 375.

Gossler, A. 2001 Moving Least-Squares: a numerical differentiation method for irregularly spaced calculation points. *Tech. Rep.*. Sandia National Laboratories, Livermore.

Hickel, S., Adams, N. A. & Domaradzki, J. A. 2006 An adaptive local deconvolution method for implicit LES. *J Comput Phys* **213** (1), 413–436.

Holm, D. D. 1999 Fluctuation effects on 3D Lagrangian mean and Eulerian mean fluid motion. *Phys D: Nonlinear Phenom* **133** (1-4), 215–269.

Hu, X. & Adams, N. 2006 A multi-phase SPH method for macroscopic and mesoscopic flows. *J Comput Phys* **213** (2), 844–861.

Hu, X. Y. & Adams, N. A. 2007 An incompressible multi-phase SPH method. *J Comput Phys* **227** (1), 264–278.

Hu, X. Y. & Adams, N. A. 2012 A SPH model for incompressible turbulence p. 23.

Lucy, L. B. 1977 A numerical approach to the testing of the fission hypothesis. *Astron.J.* **82** (12), 1013–1024.

Mansour, J. 2007 SPH and $\alpha$-SPH: Applications and Analysis. Phd thesis, Monash University.

Monaghan, J. J. 1989 On the problem of penetration in particle methods. *J Comput Phys* **82** (1), 1–15.

Monaghan, J. J. 2002 SPH compressible turbulence. *Mon Not R Astron Soc* **335** (3), 843–852.

Monaghan, J. J. 2005 Smoothed particle hydrodynamics. *Rep Prog Phys* **68** (8), 1703–1759.

Morris, J. P., Fox, P. J. & Zhu, Y. 1997 Modeling low Reynolds number incompressible flows using SPH. *J Comput Phys* **136** (1), 214–226.

Price, D. J. 2007 SPLASH: An interactive visualisation tool for Smoothed Particle Hydrodynamics simulations. *Pub Astron Soc Australia* **24**, 159–173.

Robinson, M. & Monaghan, J. J. 2012 Direct numerical simulation of decaying two-dimensional turbulence in a no-slip square box using smoothed particle hydrodynamics. *Int J Num Meth Fluids* **70** (1), 37–55.

Shi, Y., Ellero, M. & Adams, N. 2012 Analysis of intermittency in under-resolved smoothed-particle-hydrodynamics direct numerical simulations of forced compressible turbulence. *Phys Rev E* **85** (3).

Violeau, D. & Issa, R. 2007 Numerical modelling of complex turbulent free-surface flows with the SPH method: an overview. *Int J Num Meth Fluids* **53** (2), 277–304.